ISSN 0016-7029, Geochemistry International, 2011, Vol. 49, No. 6, pp. 568–577. © Pleiades Publishing, Ltd., 2011.
Original Russian Text © V.L. Tauson, D.N. Babkin, T.M. Pastushkova, T.S. Krasnoshchekova, E.E. Lustenberg, O.Yu. Belozerova, 2011, published in Geokhimiya, 2011, Vol. 49, No. 6, pp. 595–604.

Dualistic Distribution Coefficients of Elements in the System Mineral–Hydrothermal Solution. I. Gold Accumulation in Pyrite

V. L. Tauson, D. N. Babkin, T. M. Pastushkova, T. S. Krasnoshchekova, E. E. Lustenberg†, and O. Yu. Belozerova

Vinogradov Institute of Geochemistry, Siberian Branch, Russian Academy of Sciences, ul. Favorskogo 1a, Irkutsk, 664033 Russia

e-mail: vltauson@igc.irk.ru

Received February 25, 2010

Abstract—The use of trace elements (TE) as geochemical indicators is complicated by the dualism of their distribution coefficients D due to the additional (i.e., above the concentrations of an isomorphic component) incorporation of elements at structural defects of various nature (including the surface of the crystal). A pressing problem in this situation is to determine the true D values that pertain to the structural component of an admixture D^{str} and evaluate effects of other modes of TE occurrence. Only upon distinguishing D^{str} in the bulk coefficient D^{bulk} it is possible to evaluate the ore potential of fluid in terms of certain TE from the composition of a mineral containing the TE. Pyrite synthesized in solutions of variable pH at 450°C and 1 kbar (100 MPa) at fluid portions sampled in a trap is utilized to demonstrate the role of a surface nonautonomous phase (NP) in the incorporation of gold in this mineral. The distribution coefficient of gold between pyrite and hydrothermal solution is 0.14 for "pure" pyrite and 0.05 for As-bearing pyrite (containing 0.02–0.05 wt % As), and these coefficients for NP are 310 and 170, respectively. This increases the D^{bulk} for evenly distributed ("invisible") gold by factors of four and nine. In contrast to the results of earlier studies conducted at room temperature and pressure or parameters close to them, our data demonstrate that the accumulation of "invisible" Au in pyrite is controlled not only by reducing adsorption with the development of Au(0) particles and films but also by Au incorporation in NP developing in the surface layer of the crystal approximately 500 nm thick as chemically bound Au [most likely as Au(I)]. The possible reason for the high absorption capacity of NP is the defect (pyrrhotite-like) structure, which is not saturated with bonds of excess S and sulfoxi onions.

DOI: 10.1134/S0016702911060097

INTRODUCTION

Although the problem of dualistic distribution coefficients of trace elements was attacked for more than three decades, this issue is still poorly studied both experimentally and theoretically [1–3]. The problem is, however, directly related to such fundamental problems of geochemistry and ore-forming processes as the state of incompatible elements, the estimation of the metal potential of ore-forming fluids, and the mechanisms concentrating valuable components in mineral phases and the conditions of these processes. It was demonstrated in [4] that the compatible or incompatible behavior of elements depends on conditions and the types and concentrations of controlling defects, and this predetermines the dualistic nature of the crystal chemical behavior of trace elements and, hence, the dualism of their distribution coefficients. The quantitative evaluation of the concentrations of valuable components in ore-forming fluids is one of the pivoting problems of ore geochemistry, and approaches to its solution based on minerals of variable composition (isomorphic mixtures) and simultaneous crystallization laws were suggested fairly long ago [5, 6]. The problem seems to simplify with the transition from major to minor and trace components, because solutions (both solid and aqueous) can be regarded as infinitely diluted for minor and trace elements (ME). At the same time, TE can be incorporated in minerals according to mechanisms that differ from "normal" isomorphic exchange, are related to defects in the crystal structure, and thus come under the definition of endocrypty [4].

In addition to interaction with structural defects, two other incorporation mechanisms of TE important for incompatible elements are adsorption and the formation of nonautonomous phases on the surface [4]. The surface of a growing crystal can physically or chemically adsorb any TE species occurring in the solution. They are modified at the surface, and the crystal "utilizes" only products of their transformations compatible with its structure, whereas others are either desorbed or form their own individual phases (precipitates) or so-called nonautonomous phases (NP) on the crystal surface [4, 7]. These can be used to evaluate the TE contents of the solution because components occurring in microconcentrations do not saturate the crystal surface [7], and hence, the concentrations of

† Deceased

surface modes should exhibit a proportionality to the TE concentration in the solution similar to the law of mass action. This dependence is described by the distribution coefficient D^{sur} (or D^{np} in particular case). Hence, one should consider two distribution coefficients: one pertaining to the concentration of the structural mode alone and written as $D^{str}_{TE} = C^{str}_{TE}/C^{sol}_{TE}$ (the TE activity is assumed to be equal to its concentration) and the other with regard for surface TE accumulation and depending on additional factors of state $D^{sur}_{TE} = C^{sur}_{TE}/C^{sol}_{TE}$. Obviously, only the former distribution coefficient corresponds to the Henry low for the distribution of an admixture and can be, strictly speaking, applied in evaluating TE concentrations in ore-forming fluids. The role of the latter coefficient is no less important, because this coefficient depends on certain additional parameters to which the "structural" coefficient can be insusceptible. Moreover, it can, in certain instances, provide insight into the enrichment of mineral material in rare and trace elements.

Experiments are usually aimed at determining bulk distribution coefficients, which can be expressed (the *TE* index is omitted) as

$$D^{bulk} = (f^V C^{str} + f^S_h C^{sur})/C^{sol}, \quad (1)$$

where f^V and f^S_h are the mass fractions ($f^V + f^S_h = 1$) of the crystal material in the volume and surface layer (of thickness h), which depend on the size and shape of the crystal. Expression (1) makes it possible to calculate C^{sur} and the corresponding distribution coefficient from data on D^{bulk} (and, correspondingly, C^{bulk}) for any size fraction of crystals of size r, if the concentration of the structural component of TE is known.

$$C^{sur} = (C^{bulk}_r - f^V C^{str})/f^S_h. \quad (2)$$

The dualistic nature of D is evident from the increase in D^{bulk} value relative to those specified by the distribution law of isomorphic components. Generally speaking, D^{sur} also comprises two constituents, which correspond to the adsorbed mode of TE and that captured by NP: D^{sorb} and D^{np}, respectively. Note that we considered only modes of TE occurrence that are distributed relatively evenly. An admixture unevenly distributed as minute inclusions of TE autonomous phases should be excluded from analysis by applying certain specialized techniques for data processing (see below).

The term *nonautonomous phases* is referred herein to real (not virtual) objects on the surface of crystals that can be identified using direct techniques and have a certain composition, stoichiometry, structure, and morphology, as well as specific features that are different in a certain manner from the features of the corresponding "major" (i.e., autonomous) phase. Inasmuch as, in contrast to the "normal" phase, NP can have a composition that varies within broader limits (including compounds that do not occur as autonomous phases), NP can serve as a "buffer" between the environment and the volume of the crystal and prevent more profound transformations of the crystal. This is likely the main reason for the preservation of minerals in oxidation zones at ore deposits and at the Earth's surface under atmospheric conditions. At the same time, NP are principally different from common adsorbed complexes, which can be readily desorbed if parameters of the system change, which pertains, first of all, to elevated temperatures (thermal desorption). Conversely, NP behave as "normal" phases but not adsorbed complexes and are subject to the fundamental principles of physicochemical analysis, such as the principles of continuity and correspondence of phase compositions [8]. The closest concept to the core meaning of NP is that of nonstoichiometric layer (NL), which develops on sulfides during their oxidation or under the effect of acid solutions on these minerals. The reason for this is the more rapid oxidation (or passage into solution) of cations than sulfur [9]. Although NL also cannot occur autonomously (without underlying crystalline material on which it can develop), in contrast to NP (in our understanding), it cannot coexist with this material but is rather an intermediate product during a certain stage of its transformation. In other words, NP develops as a relatively stable surface structure (locally equilibrated or, according to [3], forcedly equilibrated), which minimizes the possibility of transformations of the underlying material, whereas NL are likely nondifferentiated (disordered) decomposition products of this material. Nevertheless, relations between these objects are undeniable and can be the subject of a research. Finally, it can also be hypothesized that NP somehow mediates the process of crystal growth. An atomic smooth crystal face has no driving force for its growth and the incorporation of atoms adsorbed on it (at least at low supersaturation degrees). At high degrees of oversaturation, defects (for instance, vacancies) are generated, disturb regular growth, and induce the development of vicinals. An example is provided by the TEM monitoring of the development of the surface topography of rapidly growing Pd particles [10]. The 3D reconstructed NP layer lets through useful particles and thus serves as a screen by allowing atoms utilized in crystal growth to pass and keeping useless atoms out and thus becoming saturated with them.

This series of our papers is intended to illustrate the role of NP in the dualistic distribution coefficients of precious metals in the system mineral–hydrothermal solution and to distinguish between the "true" coefficients (i.e., those related to the structural component) and "surface" coefficients, which pertain to the nonautonomous phase (under our experimental conditions). This series of publications begins with a paper devoted

Table 1. Conditions and results of fluid analysis in experiments on the synthesis of Au-bearing pyrite crystals at a temperature of 450°C and pressure of 1 kbar in the crystal growth zone

No.	Starting mixture			Starting solution (wt %)	In trap after experiment			
	S/Fe, atomic ratio	wt %			Fe, wt %	As, wt %	Au, ppm	pH
		Fe	As					
D4-1	1.9	47.83	–	$NH_4Cl(9) + Na_2S(1)$	0.76	–	13.4	8.6
D4-2	1.9	47.83	5	same	0.42	0.11	10.9	8.8
D5-5	2.03	46.18	–	$NH_4Cl(9.5) + HCl(0.5)$	0.65	–	20.4	1.4
D5-6	2.03	46.18	5	same	0.58	0.26	7.3	3.6
D6-1	2.03	46.18	–	$NH_4Cl(10)$	0.69	–	7.1	2.6
D6-4	1.9	47.83	5	same	0.61	0.1	14.6	8.9

to pyrite as one of the most important gold concentrators at mineral deposits of various genetic types.

EXPERIMENTAL AND ANALYTICAL TECHNIQUES

The experiments were carried out by conventional techniques of hydrothermal thermogradient synthesis, using traps (samplers) for portions of high-temperature fluid [11]. The experiments were conducted in stainless steel autoclaves close to 200 cm^3 in volume, with inserts of VT-8 Ti alloy. The trap of the same alloy was mounted in the upper part of the insert and fixed with pin junction. The inserts were hermetically sealed with Ti choppers with refractory steel rings (self-packing seals). Elements contained in low concentrations in the solution are not retained by it at cooling to room temperature (see, for example, [7]), and it is thus senseless to analyze the quenched solution. The method of capturing portions of the fluid (supercritical hydrothermal solution) in a trap is also not devoid of disadvantages (this is, first and foremost, the violation of the requirement of isothermal conditions), but if the difference between the experimental temperature and the critical point of the aqueous salt solution is relatively small (close to ~70°C in the instance discussed herein) and the cooling rate at quenching is high enough (approximately 5°C/s), it is reasonable to believe that the bulk mass of the fluid was captured by the trap at the greatest density of the fluid, i.e., in the proximity of the experimental temperature. The temperature in the growth zone of the crystal was 450°C, the temperature difference along the autoclave wall was 15°C, and the pressure in the reaction vessel (Ti insert) was 100 MPa (1 kbar). Au was introduced into the material of the starting mixture in the form of thin foil (99.99 pure) in an amount of 1% of the total mass of the material (Fe + S ± As), which was close to 6 g. The foil (although corroded) was always identified among the experimental products after the experiments. In certain instances, the starting mixture was doped with As, and then the pyrite crystals synthesized in the experiments contained 0.02–0.05 wt % As (quantitative atomic emission data). All experiments involved an isothermal (for the homogenization of the starting mixture) and a gradient stage (which lasted for three and nine days, respectively). The experiments were terminated with the quenching of the autoclaves in running cold water. The composition of the solutions and starting mixtures, the Au, Fe, and As concentrations in the fluid captured in traps, and the pH of this fluid are reported in Table 1. Elements were analyzed by atomic absorption spectrometry on Perkin-Elmer M 503 and Analyst 800 accurate to ±5–10%. The Au concentrations in filtrates from traps were usually roughly two orders of magnitude lower that the Au concentrations analyzed after the treatment of the inner walls of the autoclave with nitrohydrochloric acid. The total Au amount recovered from the trap and normalized to the mass of the trapped solution was assumed to be identical to the Au concentration in the fluid phase under the experimental P–T parameters.

Pyrite crystals were analyzed by X-ray pholoelectron spectroscopy (XPS) and Auger electron spectroscopy (AES), scanning probe microscopy (SPM), and X-ray electron probe microanalysis (EMPA). The analyses by electron spectroscopy were conducted applying a LAS-3000 (Riber, France). The surface topography of crystals was examined using scanning multimicroscop a SSM-2000 (Russia in scanning tunnel microscopy (STM) mode and atomic force microscopy (AFM) in contact mode. The equipment and techniques of the spectroscopic and microscopic studies are described in much detail in [12]. EMP analyses were conducted on Superprobe JXA-8200 (Jeol, Japan), using unpolished samples (natural crystal faces). The surface of the crystal faces was examined using SEM in secondary and back-scattered electrons and the X-ray radiation of Fe, S, and Au. The chemical homogeneity of pyrite was examined using both energy- and wave-dispersive spectrometers (EDS and WDS, respectively). The spectra of the analytical lines of elements to be analyzed were collected at an accelerating voltage of 20 kV, beam current

of 20 nA, beam diameter 1 μm, and a counting time of 60 s, with data processing by the software of the JXA-8200 EDS microprobe. Quantitative WDS analyses were made under the same parameters, except only for the counting time of 20 s. Matrix correlations and calculation of determined element contents have been done by the ZAF-approach using quantitative analysis programme adapted in Superprobe JXA-8200 software.

Pyrite crystals were analyzed for Au, and its distinct modes of occurrence were distinguished using the technique of statistical samples of analytical data for monocrystals (SSADSC) [13, 14], which is underlain by the analysis of single crystals. Inasmuch as here we are concerned only with two modes of Au occurrence (its structural and surface modes), the simplified modification of this technique [15] can be applied. It does not allow for the uneven distribution of a mode of occurrence and for value transitions between size levels [14]. The crystals were analyzed for Au by electrothermal atomic absorption spectrometry (ETAAS), whose methodology was discussed in [13]. This technique allows analysis accurate to ±12% at a detection limit of 0.3 ppb. If faceted crystals are available, the most morphologically perfect of them are selected, and, knowing the mass (and hence, volume) of the analyzed crystal, its characteristic size is calculated. In processing the data, the whole database of Au concentrations in individual single crystals was subdivided into ranges according to crystal masses in such a manner that all ranges contained roughly equal numbers of crystals and no less that 15. Then an average concentration was determined for each range, the mean square deviation was evaluated, and values >σ were rejected. Negative values (<–σ) were not rejected, because, according to the concept adopted here [13, 14], a crystal can contain only the structural mode of a trace element, and any additional modes of the element can only increase the concentration above the value for the structural (isomorphous) mode. Because of this, low concentrations should be treated as possible (if they are not accounted for by analytical errors). A new average value $\bar{C}_{Au}$ and the corresponding crystal mass $\bar{m}$, are then determined in order to calculate, first, the average volume and characteristic size $\bar{r}$ (with regard for the morphology) and then the specific surface $\bar{S}_s$ of an average crystal in the sample.

EXPERIMENTAL RESULTS

Pyrite crystallized as cubes and parallelepipeds with edges up to approximately 2 mm in the "pure" system and as complicated polyhedrons with {111}, {100}, {110}, and {hkl} faces in the presence of As. It is hard to describe such crystals in terms of regular geometric shapes, and hence, we tried to approximate them with spheres and hemispheres of radius *r*, which was usually approximately 1 mm. Our detailed XPS, AES, and SPM led us to discover a pyrrhotite-like NP ~500 nm thick. The NP has a variable composition $Fe^{2+}[S,S_2,S_n]^{2-}$ with the predominance of S^{2-} (at relatively low sulfur fugacity values). The NP may sometimes contain minor elements and such sulfoxi anions as SO_3^{2-}, SO_4^{2-}, and $S_2O_3^{2-}$ [12], the presence of NP was involved in explanation of the effect of crystal size on trace element concentration [15]. No evenly distributed nanometer-sized or larger Au(0) particles (STM + AFM) were identified at the surface, and only AES allowed us to identify rare inclusions very unevenly distributed on the crystals. These individuals have no chances to occur in the final samplings of SSADM analysis. A challenging problem is the analysis of the surface layer of a crystal for Au because of the small thickness of this layer. The lower limit can be determined based on the EMPA data. The most reliable quantitative analyses (with analytical totals close to 100 wt %) are yielded by concentrations of 440 ± 220 ppm on average. The electron excitation region expands to a depth of approximately 10 μm into the sample, and hence, this estimate is definitely the minimum one. Recall that the limit for Au accommodation in the pyrite structure under our experimental conditions is <3 ppm [16]. The Au 4f XPS spectrum of fine fractions with the highest Au concentrations (according to ETAAS data) shows an elevated background at bond energy of 85 eV, which corresponds to the $4f_{7/2}$ peak of Au(I). Au is reliably enough identified in synthetic Ag_2S at average concentrations of 0.2–0.5 wt % (0.08–0.2 at %) [14]. The deconvolution of the spectrum makes it possible to identify Au(0) and Au(I). A specialized study indicates that the weak 4f peaks of natural pyrite (containing up to ~1 wt % Au) from the Kvartsevaya Sopka epithermal Au–Ag deposit in northeastern Russia are pronounced only in samples with Au concentrations higher than ~0.3 wt % (0.06 at %), and these peaks are only insignificantly higher than the background. Inasmuch as an Au concentration of 0.08 at % can be reliably identified (see above for Ag_2S), the value of ~0.3 wt % or ~3000 ppm can be assumed as the upper limit for the Au concentration in the NP. Higher concentrations were likely detected by XPS.

Table 2 lists ETAAS analyses of individual pyrite crystals synthesized in our experiments. The table specifies the ranges of crystal masses in the samples, the numbers of crystals in the initial and final samples (after values >σ were rejected), average size parameters, and Au concentrations. The Au concentrations is definitely inversely correlated with the size of the crystals, as was mentioned in [15]. Data from the latter publication were appended and revised in order to derive a dependence for determining Au concentrations in distinct modes not for the whole bank of samples but only for the results on individual experiments. Thereby the results of some experiments were rejected as unsuitable

Table 2. Au concentration in pyrite crystals of various size

No.*	Range of masses, mg	Number of crystals (starting–final sample)	$\bar{m}$, mg	$\bar{r}$, mm	$\bar{S}_s$, mm^2/mg	$\bar{C}_{Au} \pm \Delta$, ppm
D4-1	0.1–0.3	18–16	0.19	0.336	3.565	24.9 ± 6.0
	0.31–1	15–12	0.67	0.512	2.347	19.0 ± 8.1
	1.01–2.01	16–14	1.51	0.671	1.789	6.3 ± 1.6
	2.02–4	12–11	3.03	0.846	1.417	4.1 ± 0.8
	4.01–9	16–14	5.89	1.056	1.136	3.2 ± 0.6
	9.01–40	14–13	19.59	1.577	0.762	2.3 ± 0.7
D4-2	0.1–0.3	19–16	0.22	0.219	2.738	23.7 ± 5.2
	0.31–0.6	20–17	0.44	0.276	2.174	12.2 ± 3.3
	0.61–1.2	20–17	0.90	0.350	1.710	4.3 ± 1.8
	1.21–1.9	20–14	1.46	0.412	1.460	4.1 ± 1.5
	1.91–2.5	15–13	2.14	0.468	1.285	3.2 ± 1.3
	2.51–5.3	15–13	3.41	0.546	1.098	2.2 ± 0.7
D5-5	0.1–0.5	15–13	0.34	0.408	2.938	35.3 ± 14.4
	0.51–1.02	14–13	0.75	0.531	2.256	18.3 ± 5.0
	1.03–2	16–12	1.52	0.672	1.783	14.9 ± 5.8
	2.01–4	22–19	3.06	0.849	1.413	9.7 ± 2.5
	4.01–10	20–17	8.05	1.172	1.024	10.1 ± 2.7
	10.01–41	14–12	18.29	1.541	0.779	5.5 ± 1.3
D5-6	0.1–0.3	17–16	0.24	0.284	3.166	17.4 ± 4.6
	0.31–0.5	29–27	0.38	0.331	2.716	11.8 ± 3.0
	0.51–1	16–13	0.73	0.412	2.190	9.1 ± 3.7
	1.01–2	14–12	1.56	0.530	1.696	5.9 ± 2.1
	2.01–5.13	10–10	3.65	0.704	1.279	1.6 ± 0.6
D6-1	0.1–0.4	17–15	0.32	0.400	3.000	17.9 ± 4.5
	0.41–0.8	17–15	0.63	0.501	2.390	13.1 ± 3.7
	0.81–1.5	19–17	1.05	0.594	2.016	10.3 ± 2.2
	1.51–3	19–16	2.14	0.754	1.594	8.5 ± 3.0
	3.01–6	19–16	4.30	0.951	1.262	6.0 ± 1.8
	6.01–10	17–15	7.53	1.146	1.046	2.2 ± 0.8
	10.01–40	18–12	18.38	1.543	0.777	2.0 ± 0.9
D6-4	0.1–0.2	22–18	0.14	0.237	3.779	27.5 ± 5.6
	0.21–1	18–14	0.52	0.368	2.453	7.5 ± 2.9
	1.01–2	19–17	1.40	0.511	1.757	1.8 ± 0.5
	2.01–3.5	16–16	2.73	0.639	1.409	1.4 ± 0.3
	3.51–5.2	21–17	4.14	0.734	1.226	1.2 ± 0.3

* See Table 1 for experimental conditions and concentrations of elements in solution.

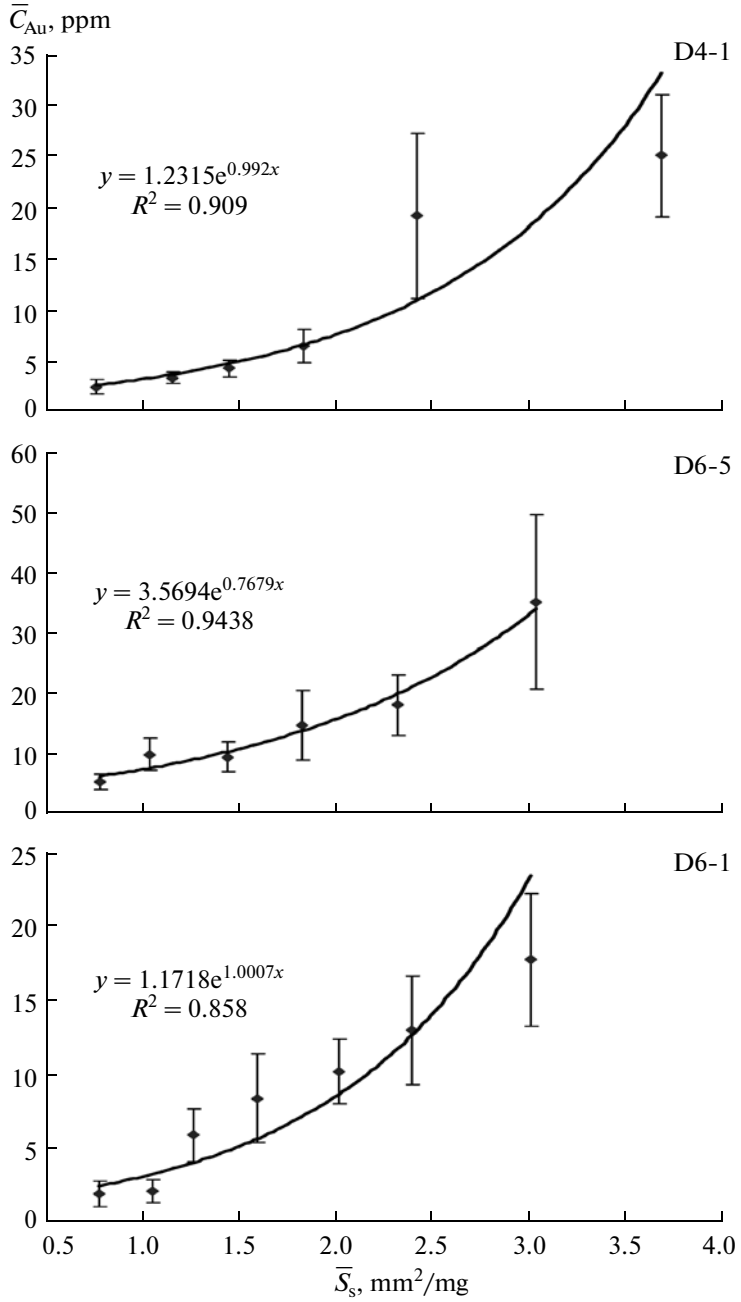

Fig. 1. Dependence of the average concentration of an evenly distributed Au admixture in pyrite samples on the specific surface area of an average crystal of a given size fraction. The value of $y(0)$ in the formulas is an estimate of the concentration refferred to the crystal volume, i.e., the structural component of the concentration.

because the lack of either data on certain size fractions (in most instances) or crystals of sufficient quality. The reproducibility of Au concentrations in the samples is ±20–45 (30% relative), which corresponds to the "natural" heterogeneity in the distribution of the structural admixture with regard for analytical error [14]. This implies that Au is contained in NP in a chemically bound state and is evenly distributed in the surface layer of the crystals. This also follows from the aforementioned XPS and EMPA data.

EVALUATION OF Au CONCENTRATIONS IN DISTINCT MODES OF AU OCCURRENCE IN PYRITE

The extrapolation of our $\overline{C}_{Au} - \overline{S}_s$ plots to $\overline{S}_s = 0$, i.e., to an "infinitely large" crystal, makes it possible to determine the concentration of the element (only its evenly distributed mode) belonging to the volume of the crystal, i.e., the structural component of the trace ele-

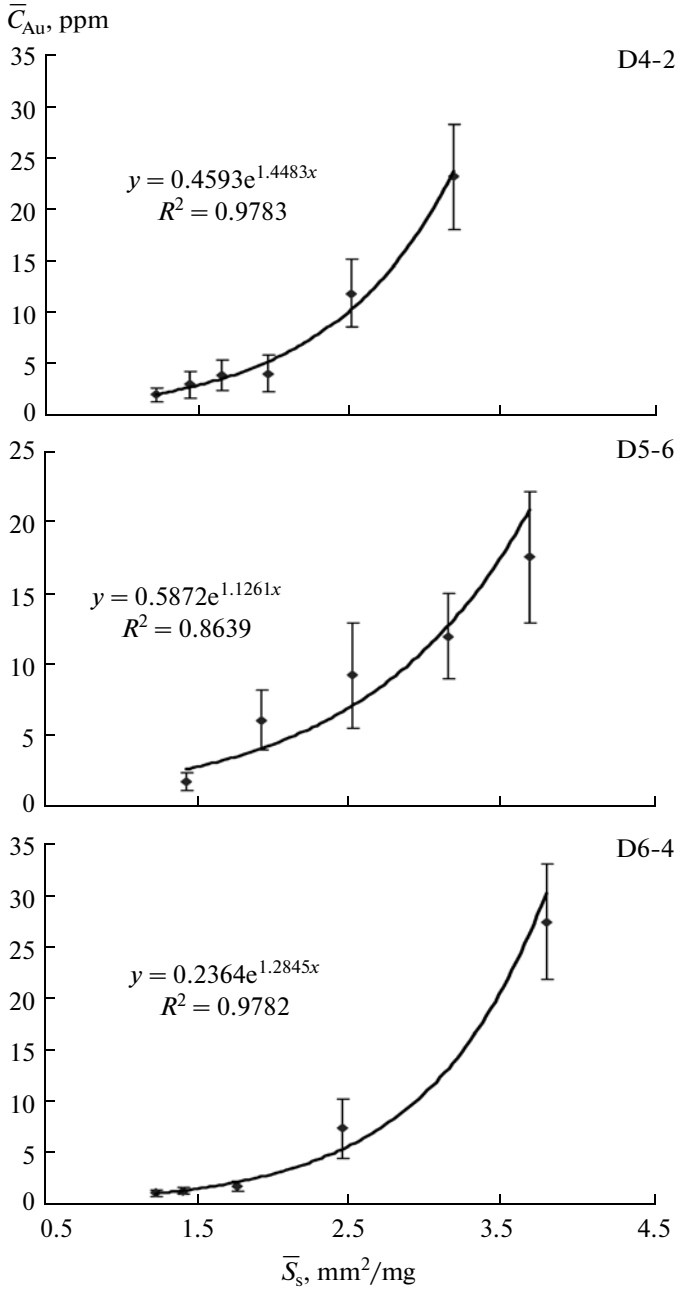

Fig. 2. Dependence of the average concentration of an evenly distributed Au admixture in As-bearing pyrite samples (0.02–0.05 wt % As) on the specific surface area of an average crystal of a given size fraction.

ment admixture C_{Au}^{str}. The corresponding plots are shown in Figs. 1 and 2 for pyrite and As-bearing pyrite, respectively, and Table 3 presents numerical values of the concentrations. The tendency of $\overline{S}_s$ toward zero according to an exponential function leads to the limit for Au accommodation in "pure" pyrite, which was demonstrated in our earlier publication [14] and means only that all surface contributions are excluded from C^{bulk}, regardless of their origin.

In order to calculate C_{Au}^{np}, parameters of NP at the surface of pyrite crystals should be specified for determining the value of f_h^S in (2). Knowing C_{Au}^{str}, one can calculate C^{sur}. According to [12], NP on pyrite has a thickness of the layer $h \cong 500$ nm (5×10^{-4} mm) and a composition close to pyrrhotite. We assumed that the phase is evenly distributed over the surface and has the density of pyrrhotite ($d = 4.7$ mg/mm^3). For a cubic pyrite crystal at $r \gg h$ (as an obvious condition, where r is the edge of the cubic crystal)

$$f_h^S = \frac{3r^3 h d_S}{(r-2h)^3 d_V}, \quad (3)$$

where r is expressed in mm, and $h = 0.0005$ mm, and d_S and d_V are the densities of the surface and volumetric phases, respectively. An analogous formula can be derived for spherical or hemispherical morphologies that approximate the habits of pyrite crystals synthesized in our experiments with the addition of As. The results of our calculations by expression (3) and an analogous formula for crystals of complicated morphology are given in Table 3, The calculations were conducted for each $\bar{r}$ of the size-fraction sample in Table 2, after which data on each experiment were averaged. The relatively high dispersion of the results is not surprising, because the development of NP depends on certain factors that were ignored in our calculations, such as the sulfur activity in the system [12]. Moreover, the scatter of masses in each sample was high enough because of the limited number of crystals of high quality falling into a given size interval in the experiments.

The calculated C_{Au}^{np} (Table 3) do not contradict our aforementioned suggestions, derived from our XPS and EMPA results, that the Au concentrations in NP should not be much higher than 0.06 at % (~ 3000 ppm). This implies that we have principally accurately evaluated the absorption capacity of NP with respect to Au. The bulk Au concentrations in samples after individual experiments were derived from the data of Table 2

$$C_{Au}^{bulk} = \sum \overline{C}_{Au}^{s} n^s \overline{m}^s / \sum n^s \overline{m}^s, \quad (4)$$

where $\overline{C}_{Au}^{s}$ is an average for each sample, and n^s and $\overline{m}^s$ are the numbers of crystals and the mass of an average crystal is this sample. To obtain comparable results of individual experiments, we excluded the largest fraction $\bar{r} \sim 1.5$ mm, which disturbs the distribution statistics. As can be seen from Table 3, the contribution of NP increases D^{bulk} relative to D^{str} by factors of four to nine, in spite of the relatively low mass fraction

Table 3. Au concentrations and distribution coefficients for the structural and surface (in NP) modes of Au occurrence in pyrite and As-bearing pyrite

no.	C_{Au}^{bulk}, ppm [a]	C_{Au}^{str}, ppm [b]	$C_{Au}^{np} \pm \Delta$, ppm [c]	D_{Au}^{bulk}	$\overline{D}_{Au}^{bulk} \pm \Delta$	D_{Au}^{str}	$\overline{D}_{Au}^{str} \pm \Delta$	$\overline{D}_{Au}^{np}$	$\overline{D}_{Au}^{np} \pm \Delta$
pyrite									
D4-1	5.15	1.23	3380 ± 1710	0.38		0.09		250	
D5-5	11.22	3.57	5200 ± 1910	0.55	0.56 ± 0.32	0.17	0.14 ± 0.04	250	310 ± 180
D6-1	5.42	1.17	3110 ± 1200	0.76		0.16		440	
As-bearing pyrite									
D4-2	4.30	0.46	1450 ± 880	0.39		0.04		130	
D5-6	5.62	0.59	1970 ± 890	0.77	0.44 ± 0.52	0.08	0.05 ± 0.03	270	170 ± 150
D6-4	2.12	0.24	1510 ± 1470	0.15		0.02		100	

Note: [a] bulk concentration of evenly distributed Au in the sample, which was calculated from data of Table 2 by expression (4);
[b] Au concentration in the volume (structure) of the crystal, based on the extrapolation of the dependence $\overline{C}_{Au} - \overline{S}_s$ to $S_s = 0$, i.e., to "infinitely large" crystal;
[c] average Au concentration in NP calculated by Eq. (2) ± one standard deviation at 90% confidence level.

on NP, and the reproducibility of D^{bulk} is twice worse than of D^{str}.

DISCUSSION

We are not aware of any publications focused on the evaluation of Au distribution coefficients between pyrite and hydrothermal solution, particularly based on the dualistic nature of the coefficients. Estimates of these values under our experimental parameters were presented only in [16] and were based on indirect data: the true coefficient, which pertains to the structure Au mode in pyrite in the presence of As and Se was evaluated at 0.06, which is fully consistent with D_{Au}^{str} for As-pyrite (Table 3). The values of the apparent distribution coefficient of Au between pyrite and acidic sulfide solution at 200°C reported in [17] range from 4.8 to 26, i.e., are much higher than the values of $D_{Au}^{bulk} \sim 0.5$ in Table 3. It should, however, be taken into consideration that the experimental conditions were significantly different: the material used in [17] was crushed to 30–60 μm, and the phase state of the system and the pyrite surface are not known. It follows from Tables 1 and 3 that the distribution coefficient of an Au admixture in the presence of As is lower than in the pure system, and this is explained by the lower concentration of the structurally bound gold in As-pyrite. Hence, the presence of As in the system results in a certain redistribution of Au into the fluid phase, and this is associated with an increase in the fractionation coefficient of Au into NP relative to the volumetric phase ($D_{Au}^{np} / D_{Au}^{str}$). The coefficient increases from 2200 for pure pyrite to 3400 for As-bearing one, which confirms the surface activity of As in Au incorporation into [18]. It is currently thought, based on an Au–As correlation in natural samples, that As facilitates Au incorporation into pyrite [19] (although opposite conclusions were drawn in [20] based on observations). It is still unknown whether Au miscibility with As-pyrite is stable (if so, these data can be compared with experimental ones) or metastable. Even in scarce papers in which the Au state was determined by direct techniques, "an unknown Au–As–S compound in which tetracoordinated Au^{1+} is bounded in fourfold coordination to sulfure and arsenic atoms [21] could be a masking factor. It was also hypothesized that the unusually high Au concentration in As-bearing pyrite can be explained by lamellae of As- and Au-bearing marcasite or Au-bearing arsenopyrite [22]. Furthermore, it is known that Au can be accommodated in the form of submicroscopically sized inclusions in As-enriched surface of pyrite crystals and in arsenopyrite [23]. These issues require further research, including the obtaining of equilibrium data on the Fe–S–As–Au system. Here we attract attention to the fact that NP plays a notable (or even determining) role in Au accumulation during the growth of pyrite crystals both in the presence and in the absence of As. This is responsible for the dualism of the distribution coefficient in the system in question: Au fractionation in NP results in an increase in the bulk distribution coefficient by several times compared to that for the structural mode of occurrence of the element.

Following the first publications of data on surface spectroscopy [24, 25], Au adsorption on the surface of sulfide minerals, including pyrite, was practically always thought to result from reducing adsorption [26–31]. However, most of the studies were carried out at room temperature (or temperatures close to it), using the surface of fractures (cuts) or crushed (pulverized)

samples of natural crystals, i.e., those with unrelaxed and unequilibrated surfaces. Moreover, as was mentioned in [17], these studies were carried out mostly with the use of solutions with the $AuCl_4^-$, anion, "which very little corresponds to the redox parameters of hydrothermal processes". Under hydrothermal conditions, the surface is chemically modified and contains an nonautonomous phase and defects, which facilitate the accommodation of admixtures. The mechanisms of admixture accommodation that should operate at elevated temperatures and pressures and under the effect of chemically aggressive supercritical fluid are more efficient than the known mechanism of surface complexation. These mechanisms involve the formation of complexes of impurity atoms with surface crystal defects and the accommodation of admixture elements in surface nonautonompous phases [4, 7]. The experimental and analytical data reported above show that Au is contained in NP in a chemically bound state and is evenly distributed in the surface layer of the crystal with depth. It is most likely that Au is contained in NP as Au(I) (see also [17]). The high adsorption capacity of NP can be related to its "loose" structure (similar to that of pyrrhotite but with a higher concentration of vacancies than in the "volumetric" phase), unsaturated bonds of excess sulfur, and sulfoxy anions.

CONCLUSIONS

We launched a research aimed at elucidating the nature of the dualism of the distribution coefficients of trace and minor elements in geochemically important systems of minerals and hydrothermal solution. The studies are carried out with the application of thremogradient crystal growth with fluid sampled by traps. The accumulation of Au by pyrite under the experimental conditions of 450°C and 1 kbar in solutions of various pH is controlled by two factors: the accommodation of the element in the structure of the nonautonomous phase that was previously discovered (with the application of several techniques) of hydrothermal pyrite crystals [12]. Statistical samples of ETAAS analytical data on individual crystals made it possible to determine Au concentrations corresponding to the aforementioned modes. Electron spectroscopic, SPM, and EPMA data suggest that Au is contained in NP in a chemically bound form [most likely Au(I)], which is evenly distributed throughout the whole depth of the surface layer of the crystals (approximately 500 nm thick). NP plays a remarkable role in Au uptake during the growth of pyrite and As-pyrite crystals. This effect is responsible for the dualism of the distribution coefficient in the system and leads to an increase in the bulk distribution coefficient by several times relative to the distribution coefficient of the structurally bound admixture. The coefficients of Au fractionation into NP relative to the "volumetric" pyrite phase is $2.2–3.4 \times 10^3$, i.e., a few thousands. The possible reason for the high adsorption capacity of NP can be its defective structure, unsaturated bonds of excess sulfur, and sulfoxy anions. In addition to the effects of capturing admixture elements, which were discovered previously [1–3], this phenomenon provides an explanation for a new concentration mechanism of incompatible elements in the course of endogenic mineral-forming processes.

ACKNOWLEDGEMENTS

The authors thank Yu.V. Shchegol'kov for help with the spectroscopic studies, S.V. Lipko for assistance in work at a scanning probe microscope, and I.E. Vasil'eva for analyses for As.

This study was financially supported by the Russian Foundation for Basic Research (project no. 09-05-00067) and the Siberian Branch of the Russian Academy of Sciences (integration projects ONZ-5.1 and 117).

REFERENCES

1. V. S. Urusov and I. F. Kravchuk, "Effect of the Entrapment of Trace Elements by Defects of Crystal Lattice and Its Geochemical Significance," Geokhimiya, No. 7, 963–978 (1978).
2. V. V. Akimov and V. L. Tauson, "Accumulation of Trace Elements in Mosaic and Micrograined Mineral Crystals: Experimental Data," Geokhimiya, No. 11, 1201–1210 (2003) [Geochem. Int. **41**, 1099–1107 (2003)].
3. V. S. Urusov, V. L. Tauson, and V. V. Akimov, *Geochemistry of the Solid* (GEOS, Moscow, 1997) [in Russian].
4. V. L. Tauson, "Systematics of Processes of Trace Element Uptake by Real Mineral Crystals," Geokhimiya, No. 2, 213–219 (2005) [Geochem. Int. **43**, 184–190 (2005)].
5. V. S. Urusov, "Energetic Formulation of Problems of Equilibrium Cocrystallization from Aqueous Solution," Geokhimiya, No. 5, 627–644 (1980).
6. L. V. Chernyshev, "To the Theory of Hydrothermal Equilibria of Minerals of Variable Composition," Geokhimiya, No. 6, 787–797 (1980).
7. V. L. Tauson, I. Yu. Parkhomenko, D. N. Babkin, et al., "Cadmium and Mercury Uptake by Galena Crystals under Hydrothermal Growth: A Spectroscopic and Element Thermo-Release Atomic Absorption Study," Eur. J. Mineral **17**, 599–610 (2005).
8. V. L. Tauson, "The Principle of Continuity of Phase Formation at Mineral Surfaces," Dokl. Akad. Nauk **425** (5), 668–673 (2009) [Dokl. Earth Sci. **425**, 471–475 (2009)].
9. A. V. Kuklinskii, Yu. L. Mikhlin, G. L. Pashkov, et al., "Conditions for the Formation of a Nonequilibrium Nonstoichiometric Layer on Pyrrhotite in Acid Solutions," Elektrokhimiya **37** (12), 1458–1465 (2001) [Russ. J. Elektrochem. **37**, 1269–1276 (2001)].
10. J. Watt, S. Cheong, M. F. Toney, et al., "Ultrafast Growth of Highly Branched Palladium Nanostructures for Catalysis," ACS Nano **4** (1), 396–402 (2010).

11. V. L. Tauson and N. V. Smagunov, "Influence of Associated Elements of Gold on Its Behavior in Fe–S–Aqueous–Salt Solution at Temperature of 450°C and Pressure of 100 MPa," Russian Geol. Geophys. **38** (3), 706–713 (1997).
12. V. L. Tauson, D. N. Babkin, E. E. Lustenberg, et al., "Surface Typochemistry of Hydrothermal Pyrite: Electron Spectroscopic and Scanning Probe Microscopic Data. I. Synthetic Pyrite," Geokhimiya, No. 6, 615–628 (2008) [Geochem. Int. **46**, 565–577 (2008)].
13. V. L. Tauson, O. I. Bessarabova, R. G. Kravtsova, et al., "On Separation of Modes of Gold Occurrences in Pyrites by Means of Studying Statistical Samplings of Analytical Data," Russian Geol. Geophys. **43** (1), 56–64 (2002).
14. V. L. Tauson and E. E. Lustenberg, "Quantitative Determination of Modes of Gold Occurrence in Minerals by the Statistical Analysis of Analytical Data Samplings," Geokhimiya, No. 4, 459–464 (2008) [Geochem. Int. **46**, 423–427 (2008)].
15. V. L. Tauson, T. M. Pastushkova, D. N. Babkin, et al., "Effect of Particle Size Variation in a Sample on Trace Element Concentration," Dokl. Akad. Nauk **429** (6), 809–815 (2009) [Dokl. Earth Sci. **429a**, 1590–1596 (2009)].
16. V. L. Tauson, T. M. Pastushkova, and O. I. Bessarabova, "On the Limit and Modes of Gold Incorporation in the Hydrothermal Pyrite," Russian Geol. Geophys. **39** (7), 932–940 (1998).
17. Yu. V. Laptev and K. B. Rozov, "Interaction of Gold with Sulfide Surface as a Factor of Its Concentration in Hydrothermal Ore Formation," Dokl. Akad. Nauk **410** (5), 663–667 (2006) [Dokl. Earth Sci. 410, 1229—1232 (2006)].
18. P. Möller, "Accumulation of Gold on Natural Sulfides: The Electrochemical Function of Arsenic in Nature," Geol. Jb. **D100**, 639–660 (1994).
19. M. Reich, S. E. Kesler, S. Utsunomiya, et al., "Solubility of Gold in Arsenian Pyrite," Geochim. Cosmochim. Acta **69**, 2781–2796 (2005).
20. P. G. Spry, S. Chryssoulis, and C. G. Ryan, "Process Mineralogy of Gold: Gold from Tellurium-Bearing Ores," J. Miner., Met., Mater. Soc. **56**, 60–62 (2004).
21. G. Simon, H. Huang, J. E. Penner-Hahn, et al., "Oxidation State of Gold and Arsenic in Gold-Bearing Arsenian Pyrite," Am. Mineral. **84**, 1071–1079 (1999).
22. D. W. Pals, P. G. Spry, and S. Chryssoulis, "Invisible Gold and Tellurium in Arsenic-Rich Pyrite from the Emperor Gold Deposit, Fiji: Implications for Gold Distribution and Deposition," Econ. Geol. **98**, 479–493 (2003).
23. S. H. McClenaghan, D. R. Lentz, and L. J. Cabri, "Abundance and Speciation of Gold in Massive Sulfides of the Bathurst Mining Camp, New Brunswick, Canada," Can. Mineral. **42**, 851–871 (2004).
24. G. Bancroft and G. Jean, "Gold Deposition at Low Temperature on Sulfide Minerals," Nature **298** (5876), 730–731 (1982).
25. G. M. Bancroft and M. E. Hyland, "Spectroscopic Studies of Adsorption/Reduction Reactions of Aqueous Metal Complexes on Sulfide Surfaces," Rev. Mineral. **23**, 511–558 (1990).
26. G. E. Jean and G. M. Bancroft, "An XPS and SEM Study of Gold Deposition at Low Temperatures on Sulphide Mineral Surfaces: Concentration of Gold by Adsorption/Reduction," Geochim. Cosmochim. Acta **49**, 979–987 (1985).
27. S. V. Kozerenko, A. M. Tuzova, I. M. Rodionova, et al., "One of the Mechanisms for the Formation of Finely Dispersed Gold in Iron Sulfides," Geokhimiya, No. 12, 1706–1714 (1986).
28. J. R. Mycroft, G. M. Bancroft, N. S. McIntyre, and J. W. Lorimer, "Spontaneous Deposition of Gold on Pyrite from Solutions Containing Au(III) and Au(I) Chlorides. Part I: A Surface Study," Geochim. Cosmochim. Acta **59**, 3351–3365 (1995).
29. M. J. Scaini, G. M. Bancroft, and S. W. Knipe, "An XPS, AES, and SEM Study of the Interactions of Gold and Silver Chloride Species with PbS and FeS2: Comparison to Natural Samples," Geochim. Cosmochim. Acta **61**, 1223–1231 (1997).
30. L. M. Maddox, G. M. Bancroft, M. J. Scaini, and J. W. Lorimer, "Invisible Gold: Comparison of Au Deposition on Pyrite and Arsenopyrite," Am. Mineral. **83**, 1240–1245 (1998).
31. Yu. L. Mikhlin and A. S. Romanchenko, "Gold Deposition on Pyrite and the Common Sulfide Minerals: An STM/STS and SR-XPS Study of Surface Reactions and Au Nanoparticles," Geochim. Cosmochim. Acta **71**, 5985–6001 (2007).